Shear Excitation of Gravity Waves. Part I: Modes of a Two-Scale Atmosphere

G. CHIMONAS

Georgia Institute of Technology, Atlanta, GA 30332

J. R. GRANT

Gould Defense Systems, Inc., Middletown, RI 02840

(Manuscript received 6 February 1984, in final form 17 May 1984)

ABSTRACT

The stabilities of two model tropospheric jets are compared. The first jet is a simple, smooth, idealized profile governed by a single scale length of tropospheric dimensions. The second jet takes the first model flow and superimposes on it a localized deformation of much smaller scale. In this second model, the shears deriving from the small-scale structure provide the subcritical Richardson numbers that support instability. The two-scale model produces a much wider range of wave instabilities. Its Kelvin–Helmholtz waves span a wavenumber domain that is nearly two orders of magnitude wider than the domain of the one-scale model, while the gravity shear waves fill out into the small wavenumber areas of the stability diagrams. However, the growth rates of the instabilities displace significantly toward smaller scales in the two-scale model.

It is suggested that the two-scale model is probably geophysically more realistic, and removes the necessity for deep layers of subcritical Richardson numbers, making it more in agreement with radiosonde observations than are smooth one-scale models.

1. Introduction

A considerable part of the wave activity in the atmosphere can be related to shear instability of the mean winds. Wave patterns in cloud layers are observed to duplicate the structure and evolution of Kelvin–Helmholtz waves generated in laboratory tanks. Similar wave forms can be identified in acoustic sounder records obtained for the nighttime boundary layer, and FM/CW radars provide beautifully detailed wave structures in the lower part of the troposphere. Aircraft probing of CAT demonstrates the presence of gravity shear waves in the turbulent regions, while tropospheric weather radars detect mesoscale waves whose properties closely match theoretical modes of an unstable wind profile. Arrays of microbarographs reveal waves that are clearly related to shear instabilities of nocturnal boundary-layer winds and upper tropospheric jets. Overall, there is a very satisfying qualitative agreement between observation and theory. The results of linear stability work explain many of the general features displayed by these natural phenomena. (Drazin and Howard, 1966; Hazel, 1972; Miles and Howard, 1964; Thorpe, 1969; Metcalf and Atlas, 1973; Gossard *et al.*, 1973; Herron and Tolstoy, 1969; Reed and Hardy, 1972; Hooke and Hardy, 1975; Mastrantonio *et al.*, 1976; Merrill, 1977; Turner, 1973).

Of course, some of the quantitative details of linearized theory, and almost all aspects of nonlinear stability theory, remain unresolved. In this paper we investigate a linear problem—how the distribution of instabilities in wavenumber space can be radically altered as the mean wind is made more complex. In Part II (Chimonas and Grant, 1984, this issue) we proceed to a nonlinear aspect, and study a mechanism by which the fast growing Kelvin–Helmholtz waves excite the longer wavelength gravity shear waves.

Our linear stability problem concerns the role played by the fine structure of an atmospheric (or oceanic) velocity profile. When investigators attempt to relate theory and observation by performing model calculations, there is always the problem of defining the mean wind field to be used. Actual radiosonde, aircraft or tower data always provide profiles which contain structure on scales down to the limits imposed by data handling. There is no way of knowing what part of this structure really pertains to the mean state, and what part derives from noise, turbulence, transient disturbances or measurement errors. Consequently, there is a tendency to smooth the data and perform stability calculations with profiles that retain only the dominant scales of the region being modeled. Thus, in boundary-layer investigations, only scales comparable with the depth of the inversion are retained, while in tropospheric studies the wind is modeled as a smooth jet with a half-width of many kilometers. There is little doubt that this approach is too conservative, and suppresses part of the real structure of the mean profile. The oceanic investigations of

Woods (1969) and the laboratory/theoretical work of J. C. R. Hunt and his co-workers (e.g., Puttock, 1976), demonstrate that the density profile of a stratified fluid contains many "steps" and "sheets." Wind profiles obtained from tall towers suggest that the atmospheric wind contains similar structures.

This structure can have a considerable influence on the model stability calculations. One of the well defined restraints of linearized stability theory is the Miles–Howard Richardson number criterion. This states that if the Richardson number everywhere within the flow is greater than ¼, the flow is stable against infinitesimal perturbations. In fact, to produce instabilities that grow at a physically acceptable rate it is necessary to have local Richardson numbers noticeably less than ¼. Consequently, the model calculations that produce instabilities on smoothed flow profiles also produce rather deep layers in which the Richardson number is below ¼. But deep-layer averaged Richardson numbers this small are not observed. Some argument can be made that the measurements, particularly of the temperature, are so inaccurate that these small Richardson numbers are masked by errors. However, it is more in keeping with the nature of the profiles to suggest that the subcritical (less than ¼) Richardson numbers are confined to small height intervals in which the local gradients are significantly different from the deep layer averages.

If this is so, it becomes necessary to use models that contain two very different scale lengths. One length will reflect the mesoscale dimension of the problem, such as the depth of the nocturnal inversion, or the half width of the tropospheric jet. The other length will provide the scale for subcritical Richardson numbers and will be much smaller. In boundary-layer work, the smaller scale may derive from the capping layer depth, or from internal structural scales whose origins and dynamics remain to be discovered. In general tropospheric models it may derive from a vertical scale associated with some prior critical layer wave absorption, or an interface that separates air masses of different origins.

One immediate and obvious question is, how does the spectrum of instabilities in a two-scale model differ from that in the simpler one-scale model? In this paper we show that these differences are considerable. The two-scale model favors the growth of Kelvin–Helmholtz small scale waves and suppresses the growth of longer scale gravity shear waves. However, the two-layer model also greatly broadens the wavenumber domain of instabilities. The Kelvin–Helmholtz family is extended to much higher wavenumbers, and, somewhat perversely, the long gravity shear waves extend over a greater area of the stability diagrams even though their growth rates are much reduced.

The two-scale linearized model aggravates a problem already present in the standard stability calculations, namely the difficulty of obtaining physically meaningful growth rates for the gravity shear waves vis-a-vis the Kelvin–Helmholtz waves. (Excellent discussions of this problem are given by Davis and Peltier, 1979, and Fritts, 1982.) In Part II we consider a nonlinear interaction of the Kelvin–Helmholtz modes that resonantly forces the appearance of the gravity shear waves. The two-scale model is a very effective basis for this interaction.

2. The two-scale model

Figure 1 shows the large scale temperature and wind structure used in our calculations. These profiles

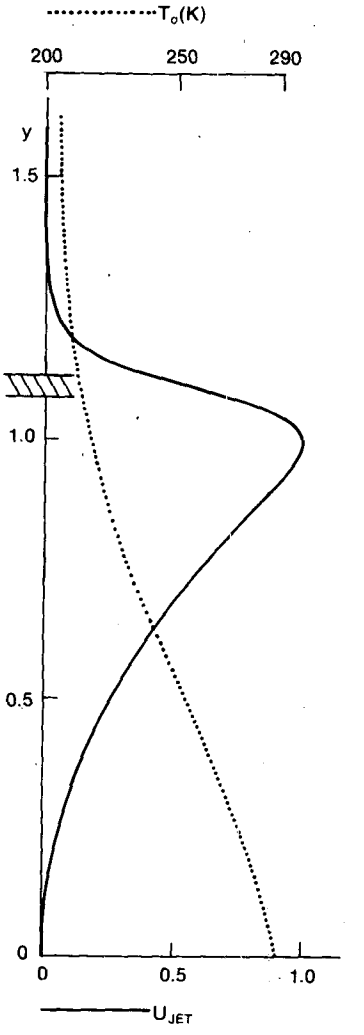

FIG. 1. Profiles of temperature and jet speed (U_{JET}) used to describe the tropospheric scale variations in the model (after Mastrantonio *et al.*, 1976). The thin hatched interval is ten times the height interval L associated with the kink [Eq. (3)], indicating the vast differences in scales involved.

are taken from Mastrantonio *et al.* (1976). They are reasonable facsimilies of the tropospheric jet, and have the simple and convenient analytic forms

$$\text{Temperature} = T(y) = T_\infty + \Delta T\{1 + \exp[2k_T(y - y_0)]\}^{-1}, \quad (1)$$

$$\text{Jet Speed} = VU_{\text{JET}}(y) = V(m_1/m_2)y^{m_2}\{y^{m_1} + [(m_1 - m_2)/m_2]\}^{-1}, \quad (2)$$

where the variable y is the height above ground normalized by a scale H, and V is a scaling factor for the velocity that allows us to change the model shears and Richardson numbers. All other parameters are fixed throughout at the values $H = 12$ km, $T_\infty = 203$ K, $\Delta T = 100$ K, $k_T = 18$, $y_0 = 0.5$, $m_1 = 30$ and $m_2 = 2$. This part of the background varies only on scales comparable with the depth of the troposphere.

A second, very different, scale is introduced by adding a local variation to the wind speed:

$$\text{kink velocity} = u_{\text{KINK}} = Vu_k\{1 + H^2(y - y_k)^2L^{-2}\}^{-1}, \quad (3)$$

where $u_k = -0.05$, $y_k = 1.1$ and $L = 50$ m.

A standard radiosonde could not detect variations with these scales and amplitudes. They are only revealed in the upper troposphere by special high resolution experiments (e.g., Axford, 1968). In the boundary layer, accurate profiles are available from instrumented towers, and such small scale variations are routinely observed. It seems reasonable that atmospheric flows will generally include small scale structures of this type.

This small localized flow detail has significant consequences. With it, we can obtain unstable Richardson numbers when the large scale part of the profile alone would predict stability. It is important, when comparing theory and observation, to recognize this. The normal radiosonde data often lead to an apparent conflict between stability theory and measured wave characteristics. The "hidden" small scale features can resolve such discrepancies. Furthermore, the kink introduces a scale that allows an entire range of small scale instabilities not found with the smooth jet profiles.

We have indicated in Fig. 1 the location of this kink, but it is impractical to attempt to draw this small anomaly on the large scale profile.

3. Linearized stability theory

Linearized stability calculations have been extensively reported in the literature, and so technical details will be kept to a minimum here. Our interest is in the results of such calculations applied to a two-scale model, not the numerical procedures. However, some discussion must be given to the technique used at large wavenumbers where a "local" calculation is needed to avoid the numerical swamping encountered in the full model.

All disturbances are taken to be two dimensional. A horizontal direction x, defined to be coincident with the direction of the winds (2) and (3), defines the (x, y) plane of the calculations. Perturbation fields are taken to have a harmonic time and x dependence, $\exp i\{\omega t - kx\}$. Then Euler's equations, conservation of mass and the adiabatic gas law are linearized in perturbation amplitudes and manipulated (Einaudi and Lalas, 1974; Davis and Peltier, 1976) to give an eigenvalue equation for ω. It is well established that as long as the horizontal phase velocity of the wave is much less than the speed of sound, the Taylor–Goldstein equation provides a highly accurate simplified form of the eigenvalue equation:

$$\phi'' + [J\alpha^2\beta(y)\Omega^{-2}(y) + \alpha U''(y)\Omega^{-1}(y) - \alpha^2]\phi = 0. \quad (4)$$

Here, a prime denotes a derivative with respect to y; U is the wind speed;

$$\phi = \bar{\rho}^{1/2}w, \quad (5)$$

where w is the vertical component of fluid velocity;

$$\alpha = kH \quad (6)$$

is a normalized wavenumber;

$$\beta = -[(\bar{\rho}'/\bar{\rho}) + (J/\bar{C}^2)] \quad (7)$$

is a nondimensionalized Brunt–Väisälä frequency in which $\bar{C}$ is the normalized sound speed;

$$J = gHV^{-2}, \quad (8)$$

and Ω is a nondimensionalized intrinsic frequency given by

$$\Omega = (\omega HV^{-1} - \alpha U). \quad (9)$$

When we add the two boundary conditions

$$\phi(0) = 0 = \phi(\infty), \quad (10)$$

as is appropriate for the atmospheric problem with complex ω corresponding to growth, we obtain an eigenvalue problem in ω. The flow field U in these equations is U_{JET} when we examine the smooth profile system and $U_{\text{JET}} + u_{\text{KINK}}$ when we deal with the more general problem.

It is useful to have a parameter characterizing the stability (or, more appropriately, the instability) of a given flow. The minimum Richardson number within the flow, J_0, is usually assigned this role, and we shall follow this convenient custom. This is a gradient Richardson number, defined as

$$J_0 = J[\beta U'^{-2}]_{\text{MIN}}. \quad (11)$$

Our numerical routines for solving this eigenvalue problem were obtained from F. Einaudi and co-

workers who have developed and tested them in a series of applications (Lalas and Einaudi, 1976; Fua *et al.*, 1976; Mastrantonio *et al.*, 1976). Applying them to the present problem, we obtain growth rates and stability boundaries for the longer wavelength ($\alpha < 20$) instabilities of the flow.

The large wavenumber instabilities introduce a computational problem. For α greater than about 20, the routines cannot integrate the equations over the full tropospheric depth because the exponential factors associated with solutions produce numerical swamping. But this is a regime of Kelvin–Helmholtz waves localized to a small height interval about their critical levels. An appropriate local form of the stability theory can be employed. The critical level is always near y_k [see (3)], and these modes experience the jet profile only as an almost constant mean linear shear in a flow with an almost constant Brunt–Väisälä frequency. Hence, we may set

$$U(y) = u_{\mathrm{KINK}}(y) + U_{\mathrm{JET}}(y_k) + (y - y_k)U'_{\mathrm{JET}}(y_k), \quad (12)$$

$$\beta(y) = \beta(y_k). \quad (13)$$

As $[(y - y_k)H/L^2]^2$ becomes large, u_{KINK} falls to zero, and with the approximations (12) and (13), (4) takes a standard form

$$\frac{d^2\phi}{d\zeta^2} + (R\zeta^{-2} - 1)\phi = 0. \quad (14)$$

We have used the coordinate transformation

$$\zeta = \alpha\{y - y_k + [\omega - \alpha U_{\mathrm{JET}}(y_k)][\alpha U'_{\mathrm{JET}}(y_k)]^{-1}\} \quad (15)$$

and the constant

$$R = J\beta U'^{-2}_{\mathrm{JET}}(y_k). \quad (16)$$

The general solution of (14) is

$$\phi = \zeta^{1/2}[AK_\nu(\zeta) + BI_\nu(\zeta)], \quad (17)$$

$$\nu^2 = 0.25 - R, \quad (18)$$

and K_ν and I_ν are Modified Bessel functions. In the limit $\zeta \to \infty$,

$$K_\nu(\zeta) \to (\pi/2\zeta)^{1/2} \exp\{-\zeta\}, \quad (19)$$

$$I_\nu(\zeta) \to (2\pi\zeta)^{-1/2} \exp\{\zeta\}. \quad (20)$$

Only the first of these is appropriate behavior for a localized instability. Thus, an eigensolution must have the behavior

$$\frac{\phi'}{\phi} \to \alpha\left[K_\nu^{-1}\frac{d}{d\zeta}K_\nu + \frac{1}{2}\zeta^{-1}\right] \quad \text{as} \quad \zeta \to \infty. \quad (21)$$

A similar relationship is derived for the lower boundary conditions $\zeta \to -\infty$, and since the K_ν can be computed from known asymptotic series, a well posed eigenvalue problem is obtained.

This small scale formulation can be used from at least $\alpha = 18$ out to the largest wavenumbers of interest; the standard algorithms can be used for values of α up to about 20. The region of overlap, $18 \leqslant \alpha \leqslant 20$, in which both techniques give accurate results, allows a consistency check on the two numerical procedures.

4. Results

When the one-scale smooth jet profile, U_{JET}, is used for U in the Taylor–Goldstein equation (4), we reproduce the results of Mastrantonio *et al.* (1976). Figure 2 shows the resulting stability boundary in (α, J_0) space. The area below the bimodal curve corresponds to instability. Within it each (α, J_0) point allows one or more unstable eigenfunctions with a complex frequency ω. It is readily seen from (4) that for each unstable eigenfunction with frequency ω there is a stable complex conjugate function with frequency ω^*.

The bimodal form of the curve derives from the superposition of two single-peaked stability curves.

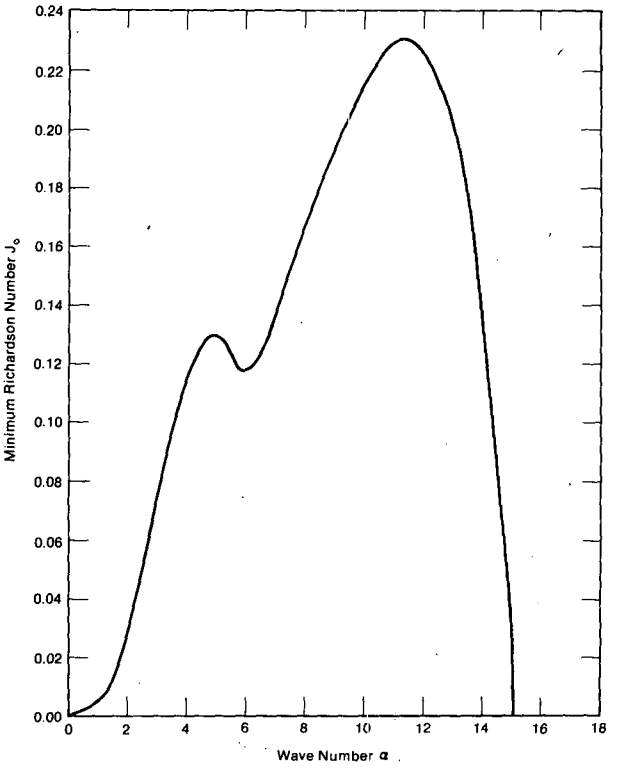

FIG. 2. The stability boundary for the profile given in Fig. 1. The coordinates are normalized wavenumber α and minimum shear Richardson number in the flow, J_0. Instabilities exist in the domain bounded by the curve and the horizontal axis.

The shorter wavelength family, peaking here at $\alpha \approx 11$, is usually identified as the Kelvin–Helmholtz branch. The longer wavelength family can be referred to as the gravity shear wave branch. In more general circumstances the gravity shear wave branch may also contain a substructure of families corresponding to harmonic sets of boundary-layer modes trapped in the lower troposphere and/or radiating modes that propagate freely into the upper atmosphere (Mastrantonio *et al.*, 1976).

It is possible to interpret the shear instability in terms of wave overreflection, an outlook that originated with Jones (1968). Davis and Peltier (1977) have made this correspondence for the boundary-layer modes with internal waves reflecting at the earth's surface (see also Rosenthal and Lindzen, 1983), and Lindzen and Rosenthal (1983) have performed a comparable analysis for Kelvin–Helmholtz waves, where all the reflections take place in the interior of the fluid.

Our concern is with the consequences of introducing a second scale in the profiles, provided here by u_{KINK}. We solve the Taylor–Goldstein eigenvalue problem for this two-scale model, and obtain the new stability curves shown in Figs. 3 and 4.

It is immediately evident that the instability structure of the two-scale model is very different from that of the single-scale model. The kink has extended the Kelvin–Helmholtz waves to higher wavenumbers. In Fig. 2, the modes cut off at $\alpha \approx 15$, but in Fig. 4 we find instabilities out to $\alpha \approx 280$.

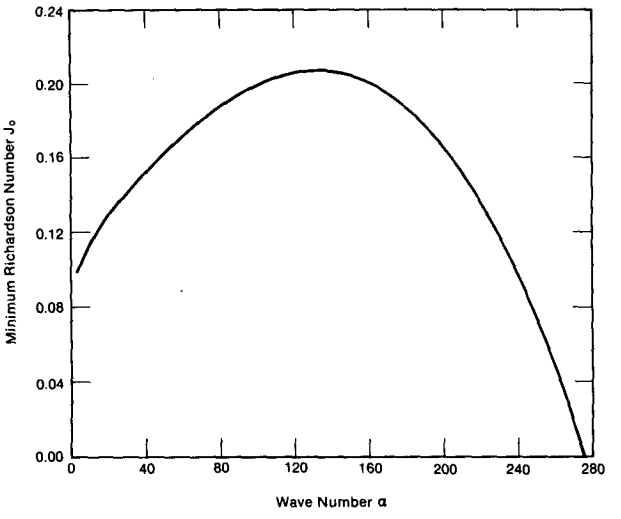

FIG. 4. Continuations of the curves of Fig. 3 to the short wavenumbers. Note that no equivalent domain exists for the smooth jet of Figs. 1 and 2.

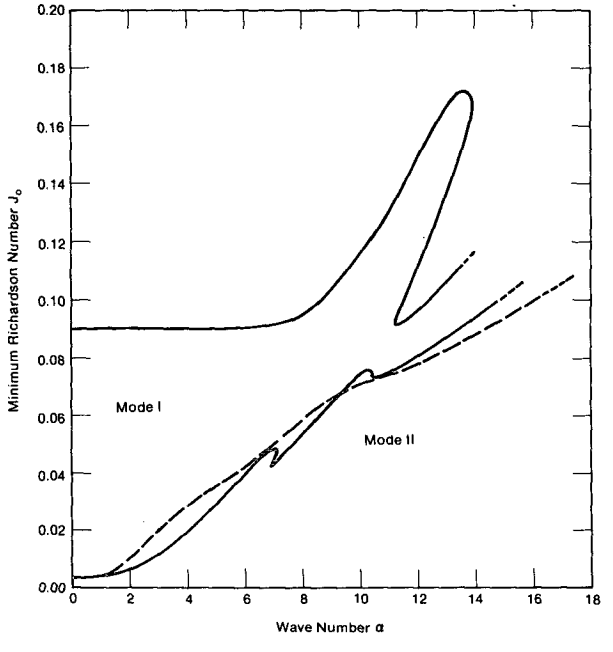

FIG. 3. Low wavenumber portion of the stability boundary for the flow obtained by combining the jet profile of Fig. 1 and the small-scale structure U_{KINK} [Eq. (3)]. Two subdomains, within which distinct modal forms I and II exist, are identified. The jet profile contributes only a minor part of the shear at the most unstable height, so that if the small-scale structure is removed the parameter J_0 increases by a factor of 4.

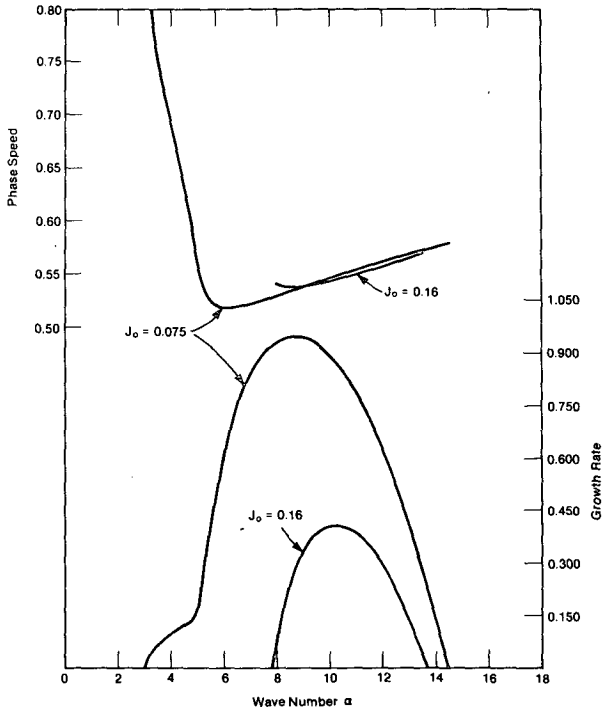

FIG. 5. Normalized growth rates αCi (lower) and phase speed Cr (upper) for the instabilities of the smooth jet profile alone. Equivalent expressions are αCi = (imaginary part ω) $\times$ H/V and Cr = (real part ω)/(kV).

Miles and Howard (1964) first established a connection between a scale in the mean flow and the scale of the instabilities. They analyzed a piecewise continuous profile with a shear layer of depth $2h$ set between unbounded homogeneous layers. They discovered that the most unstable wave had wavenumber $\hat{k}$ such that $\hat{k}2h \approx 1$. Hazel (1972) obtained similar results: using the flow $U = \tanh(y/h)$, he also established that maximum growth occurs for wavenumbers $\hat{k}$ such that $\hat{k}2h \approx 1$.

Similar results hold here. The growth rates for the instabilities are shown in Fig. 5 (for the one-scale smooth jet), and Figs. 6 and 7 (for the two-scale kinked profile). The Kelvin–Helmholtz growth rates of the smooth jet peak at wavenumbers between 8 and 10, depending on the Richardson number selected for study. Examining the jet profile (2), we find it peaks at $y = 1$ and has maximum shear at $y = 0.89$. This gives a depth of 0.11 for the shear region and 1/0.11, or 9 for the expected wavenumber of maximum growth rate, a result that agrees well with the results of Fig. 5. The peak in the neutral curve (Fig. 2) occurs at a similar value of k. For the kinked profile, the form (3) shows that the (normalized) second scale in this problem is $h = L/H = 1/240$. The growth rate curves (Fig. 7) peak at around $\alpha = 120$, giving $2\alpha h \approx 1$, as was found also by Hazel (1972).

Introduction of the second scale has had the easily understood consequence of extending the Kelvin–Helmholtz modes to higher wavenumbers. Comparison of Figs. 2 and 3, however, shows that it has also resulted in an extension of the gravity shear modes to lower wavenumber areas of the stability diagram. This was not anticipated, and we have not sought any detailed understanding of the result. It is probably a consequence of the smaller velocity contrast between the jet and the upper region, when the kink, rather than the smooth jet, provides the shear needed for a subcritical Richardson number.

The redistribution of growth through the wavenumber spectrum is enormous. Even with the smooth flow, U_{JET}, the Kelvin–Helmholtz modes outgrew the gravity shear modes by a factor of 10 (Fig. 5), but with the kinked profile, the factor increased to 50. This increased contrast comes largely from a reduction of the growth rate of the gravity shear waves, and only in lesser part from stronger growth of the Kelvin–Helmholtz family. If it was difficult to under-

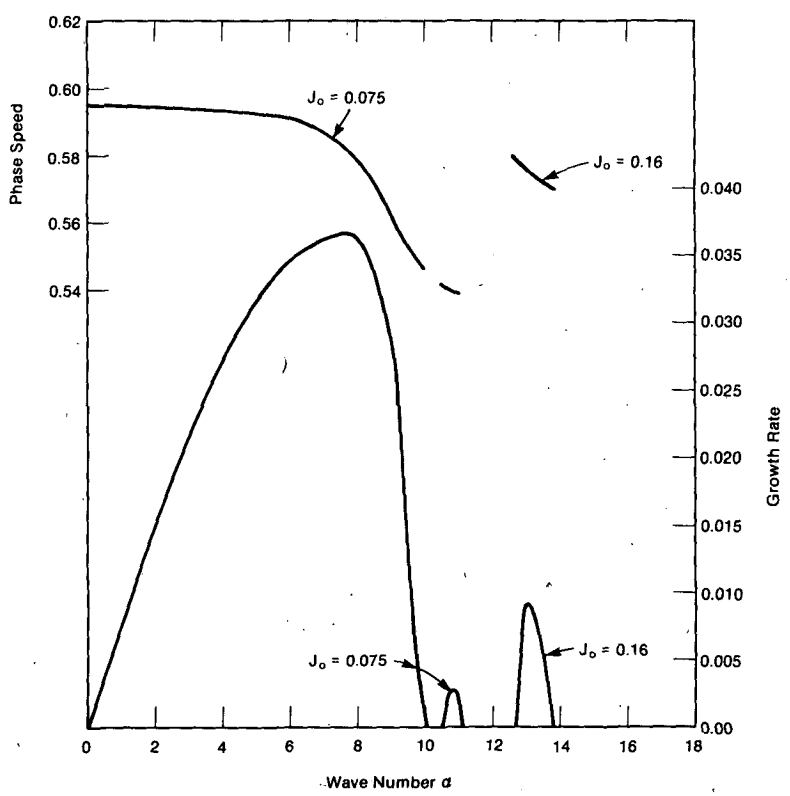

FIG. 6. Normalized growth rates αCi (lower) and phase speeds Cr (upper) for Mode I instabilities of the combined profile. These are wavenumber scans at selected values of J_0.

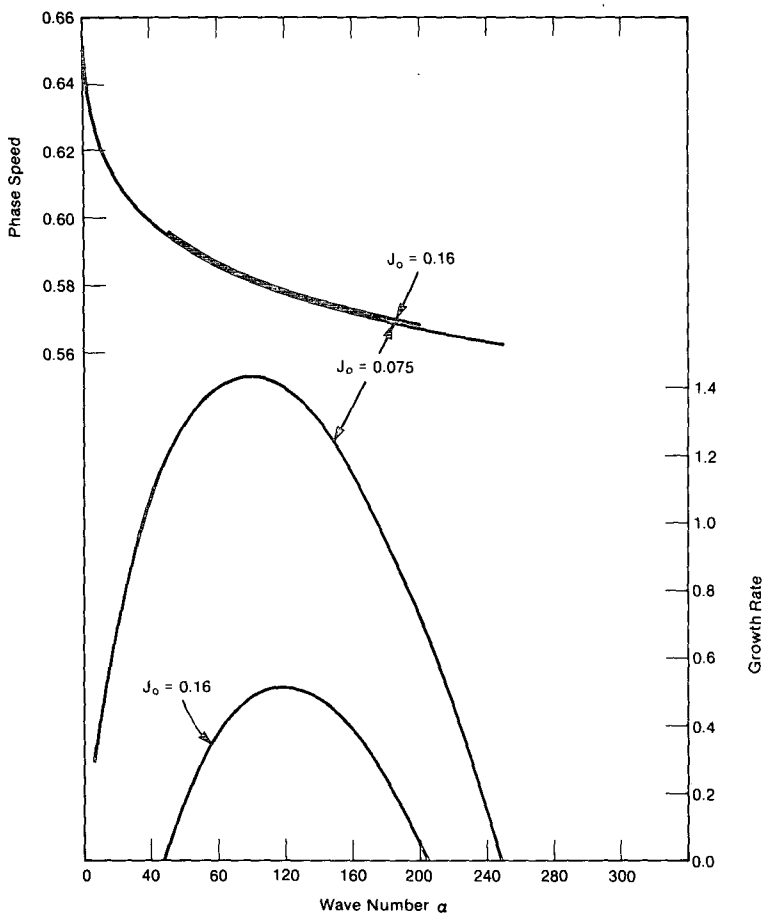

FIG. 7. As in Fig. 6 but for Mode II instabilities of the combined profile. This is the Kelvin–Helmholtz family derived from the kink on the velocity profile.

stand how the gravity shear waves could compete with the shorter scale waves in the smooth flow, the difficulty is now made more acute.

So far the results and discussion have been presented in terms of normalized scales and somewhat abstract curves. We will now discuss the physical properties scaled to a tropospheric jet.

To make the wind profile of Fig. 1 peak at the observed altitudes of ~12 km, we must take our normalization scale H [see (2) *et seq.*] to be 12 km. Then the second scale L controlling the kink profile will correspond to 50 m in the results presented here. First consider the depth of the subcritical Richardson number regions. For the smooth jet profile alone, a minimum of the Richardson number is surrounded by a layer almost 1 km deep in which the Richardson number is no more than twice this minimum value. Standard rawinsondes give temperature and velocity data at every 300 m in altitude (and have an even higher capability). Hence these soundings should certainly resolve the layers of low Richardson numbers if they occur with scales of 1 km or more. They have yet to be reported. By contrast, the kink, with a vertical scale of 50 m, would not be detectable with the standard data sets.

Also, it is easily seen why the kink, although very small in amplitude, can dominate the Richardson number

$$\mathrm{Ri} = \frac{(\text{Brunt–Väisälä frequency})^2}{(\text{Velocity Shear})^2}. \qquad (22)$$

The velocity shear to the second power in the numerator of (22) means that as we reduce the scale h of structures included in the velocity profile, their importance grows as h^{-2}. In the results presented above, the kink had an amplitude of only 5% of the amplitude of the smooth jet on which it was superimposed. However, the subcritical Richardson numbers in the kinked profiles derived almost entirely from the shears introduced by this kink. Conversely, when the kink is removed, the amplitude of the smooth jet component must be greatly increased to maintain the minimum Richardson number. This

should be borne in mind when comparing Fig. 2 with Figs. 3 and 4, or Fig. 5 with Figs. 6 and 7. The parameter J_0 may be the same in each case, but the absolute amplitude V of the jet will be very different.

This in turn influences the manner in which observed data can be modeled. Mastrantonio *et al.* (1976, Section 4) investigated a smooth jet model for an observed upper-level wave disturbance. They found it necessary to use a peak flow speed greater than that revealed by the rawinsonde, and also derived a wave phase speed greater than observed. Both discrepancies are easily removed by judicious selection of a kinked profile. In principle, the rawinsonde sensing capabilities considerably exceed the profiling sensitivities that are used on standard releases. Although such kinks presently escape detection, they are probably within the limits of available sensing systems.

The growth rates of gravity shear modes in the jet pose something of a dilemma (Davis and Peltier, 1979; Lindzen and Rosenthal, 1983). The stability diagram (Fig. 2) shows that the gravity shear wave branch only exists if the Richardson number J_0 in the flow falls below 0.13. The Kelvin–Helmholtz instabilities, on the other hand, set in as soon as J_0 falls below about 0.23. It would then be expected that, as the jet formed in response to synoptic conditions, Kelvin–Helmholtz waves would grow as soon as J_0 fell to this value. We know from laboratory work (Thorpe, 1971) that these waves break, generating vigorous turbulence and mixing. This would be expected to control the shears in the jet so that J_0 is never much below the critical value for instability. Gravity shear waves would never form, since the lower values of J_0 would never be realized.

The situation with the kinked jet (Figs. 3 and 4) appears to be even worse. It is totally unreasonable to expect synoptic conditions to produce a profile which is unstable against the longer wavenumbers, when the shorter scale instabilities provide all the turbulence needed to prevent such shears.

One possible mechanism that explains the observed existence of the gravity shear mode involves a two-stage instability. We suggest that the synoptic conditions and the mixing introduced by Kelvin–Helmholtz breakdown do indeed limit the mean jet to a smooth profile that is at most slightly subcritical. However, a local overturning of the Kelvin–Helmholtz instabilities leads (temporarily) to a local step-like structure within the jet profile. Turner (1973, p. 104) discusses how such internal mixing produces step-like structures on a density field. It is straightforward to generalize this concept to produce sharp steps in velocity and temperature within the region of Kelvin–Helmholtz roll-up, and at its boundaries. This secondary profile now contains kinks and locally small Richardson numbers. The present paper has investigated the stability of a simple version of this secondary profile. The kinks produce the low values of J_0 needed to support the gravity shear modes.

However, examining the growth rate curves (Figs. 6 and 7) shows that the gravity shear waves have very small growth rates. The very small scale Kelvin–Helmholtz waves have very large growth rates. In Part II, we present a nonlinear calculation that couples the two parts of the spectrum, allowing small scale Kelvin–Helmholtz waves to excite the gravity shear modes.

Acknowledgments. This work was funded by NOAA during 1978–80 while GC was employed by the Wave Propagation Laboratory and JRG was a graduate student at CIRES. It was completed with support from the National Science Foundation under Grant ATM-8317367. The authors received extensive helpful comments from unidentified referees.

REFERENCES

Axford, D. N., 1968: On the accuracy of wind measurements using an inertial platform in an aircraft, and an example of measurement of the vertical mesostructure of the atmosphere. *J. Appl. Meteor.*, **7**, 645–666.

Chimonas, G., and J. R. Grant, 1984: Shear excitation of gravity waves. Part II: Upscale scattering from Kelvin–Helmholtz waves. *J. Atmos. Sci.*, **41**, 2278–2288.

Davis, P. A., and W. R. Peltier, 1976: Resonant parallel shear instability in the stably stratified planetary boundary layer. *J. Atmos. Sci.*, **33**, 1287–1300.

——, and ——, 1977: Effects of dissipation on parallel shear instability near the ground. *J. Atmos. Sci.*, **34**, 1868–1884.

——, and ——, 1979: Some characteristics of the Kelvin–Helmholtz and resonant overreflection modes of shear flow instability and of their interaction through vortex pairing. *J. Atmos. Sci.*, **36**, 2394–2412.

Drazin, P. G., and L. N. Howard, 1966: Hydrodynamic stability of parallel flow of inviscid fluid. *Advances in Applied Mechanics*, Vol. 9, Academic Press, 1–89.

Einaudi, F., and D. P. Lalas, 1974: Some new properties of Kelvin–Helmholtz waves in an atmosphere with and without condensation effects. *J. Atmos. Sci.*, **31**, 1995–2007.

Fritts, D. C., 1982: Shear excitation of atmospheric gravity waves. *J. Atmos. Sci.*, **39**, 1936–1952.

Fua, D., F. Einaudi and D. P. Lalas, 1976: The stability analysis of an inflexion-free velocity profile and its application to the night time boundary layer in the atmosphere. *Bound.-Layer Meteor.*, **10**, 35–54.

Gossard, E. E., J. H. Richter and D. R. Jensen, 1973: Effect of wind shear on atmospheric wave instabilities revealed by FM/CW radar observations. *Bound.-Layer Meteor.*, **4**, 113–131.

Hazel, P., 1972: Numerical studies of the stability of inviscid stratified shear flows. *J. Fluid Mech.*, **51**, 39–61.

Herron, T. J., and I. Tolstoy, 1969: Tracking jet stream winds from ground level pressure signals. *J. Atmos. Sci.*, **26**, 266–269.

Hooke, W. H., and K. R. Hardy, 1975: Further study of the atmospheric gravity waves over the Eastern Seaboard on 18 March 1969. *J. Appl. Meteor.*, **14**, 31–38.

Jones, W. L., 1968: Reflection and stability of waves in stably stratified fluids with shear flow: A numerical study. *J. Fluid Mech.*, **34**, 609–624.

Lalas, D. P., and F. Einaudi, 1976: On the characteristics of gravity waves generated by atmospheric shear layers. *J. Atmos. Sci.*, **33**, 1248–1259.

Lindzen, R. S., and A. J. Rosenthal, 1983: Instabilities in a stratified fluid having one critical level. Part III: Kelvin–Helmholtz instabilities as overreflected waves. *J. Atmos. Sci.*, **40**, 530–542.

Mastrantonio, G., F. Einaudi, D. Fua and D. P. Lalas, 1976: Generation of gravity waves by jet streams in the atmosphere. *J. Atmos. Sci.*, **33**, 1730–1738.

Merrill, J. T., 1977: Observational and theoretical study of shear instability in the air flow near the ground. *J. Atmos. Sci.*, **34**, 911–921.

Metcalf, J. I., and D. Atlas, 1973: Microscale ordered motions and atmospheric structure associated with thin echo layers in stably stratified zones. *Bound.-Layer Meteor.*, **4**, 7–36.

Miles, J. W., and L. N. Howard, 1964: Note on a heterogeneous shear flow. *J. Fluid Mech.*, **20**, 331–336.

Puttock, J. S., 1976: Turbulent diffusion in separated and stratified flows. Ph.D. dissertation, University of Cambridge.

Reed, R. J., and K. R. Hardy, 1972: A case study of persistent intense clear turbulence in an upper level frontal zone. *J. Appl. Meteor.*, **11**, 541–549.

Rosenthal, A. J., and R. S. Lindzen, 1983: Instabilities in a stratified fluid having one critical level. Part II: Explanation of gravity wave instabilities using the concept of overreflection. *J. Atmos. Sci.*, **40**, 521–529.

Thorpe, S. A., 1969: A method of producing a shear flow in a stratified fluid. *J. Fluid Mech.*, **32**, 693–704.

——, 1971: Experiments on the instability of stratified shear flows: Miscible fluids. *J. Fluid Mech.*, **46**, 299–320.

Turner, J. S., 1973: *Buoyancy Effects in Fluids.* Cambridge University Press, 104 pp.

Woods, J. D., 1969: On Richardson's number as a criterion for laminar–turbulent–laminar transitions in the ocean and atmosphere. *Radio Sci.*, *4*, 1289–1298.